International Journal of Innovative
Computing, Information and Control
Volume **19**, Number **5**, October **2023**

 ISSN 1349-4198
pp. 1471–1486

A HYBRID VISUAL EVOKED PARADIGM FOR BRAIN COMPUTER INTERFACE BASED ON THE RADIAL MOTION OF ROBOTIC ARMS

Minghua Wei

Department of Information Engineering
Fuzhou Polytechnic
No. 8, Lianrong Road, Fuzhou 350108, P. R. China
weiminhualw@163.com

Received January 2023; revised May 2023

Abstract. *Visual evoked stimulus is one of the most important paradigms for construction of brain computer interface (BCI). To improve the diversity of the visual stimulus paradigm, this paper proposes a hybrid visual evoked stimulus paradigm to simultaneously evoke event-related desynchronization (ERD) and steady-state motion visual evoked potential (SSMVEP). The hybrid visual evoked stimulus paradigm is based on the radial motion of robotic arms. The SSMVEP is generated by the periodic motion of the robotic arm modulated by the sinusoidal function, and the ERD is generated by observing the motion of robotic arms and discriminating between left and right. Six subjects were invited to participate in the experiment, and radial motions of robotic arms with six different frequencies were designed. During the experiment, the stimulus paradigms of the arm movement based on body (AMB), arm movement based on itself (AMI), and Newton rings were designed for comparison, and two different algorithms were used to analyze the ERD and SSMVEP for the recorded EEG signals, respectively. Experimental results have shown that the proposed hybrid paradigm will evoke such two phenomena with good recognition accuracy, and the recognition accuracy of the SSMVEP is significantly higher than that of the Newton rings. The results of the analysis for the fatigue and comfort questionnaire after the experiment have shown that the proposed hybrid paradigm has a higher comfort and can cope well with fatigue after a long-term use.*

Keywords: Brain computer interface, Hybrid paradigm, Steady-state motion visual evoked potential, Event-related desynchronization, Comfort and fatigue

1. **Introduction.** Brain computer interface (BCI) realizes direct control of external devices by using the recorded brain signals and bypassing the muscular system [1]. Specifically, BCI based on noninvasive electroencephalogram (EEG) signals is of considerable interest in biomedical engineering and rehabilitation [2]. Currently, EEG-based stimulus paradigms for BCI include spontaneous and evoked types of stimuli [3]. Evoked stimulus paradigms typically generate brain feedback patterns by using a specific sound task or a visual task, including event-related potential (ERP) feedback from the frontal lobe [4] and visual evoked potential (VEP) feedback from the occipital lobe [5]. A single visual stimulus can induce transient VEP (TVEP) feedback [6], and repeated visual stimuli with a fixed frequency can induce a steady-state VEP (SSVEP) feedback [7]. The stable event-related desynchronization (ERD) [8] phenomenon produced by human brain in the process of motor imagery (MI) is the main paradigm for spontaneous stimulus. In recent studies, the correlation between action observation (AO) and human mirror neuron system (hMNS)

DOI: 10.24507/ijicic.19.05.1471

demonstrated that continuous and stable observation of the human body or a humanoid robot can also generate ERD feedback by visual induction [9].

Rapid development of deep learning algorithms is increasing the recognition accuracy of the conventional BCI paradigm. Thus, the single stimulus paradigm has become a key factor that restricts the development of the BCI control system [10]. Recently, hybrid stimulus paradigm studies have been conducted, including ERP + SSVEP [11], ERP + MI [12], and SSVEP + MI [13], and the performance of the BCI control system has been significantly improved. However, the hybrid paradigm cannot settle the disadvantages of three conventional paradigms [14]:

1) Repeated ERP will lead to suppression of the cognitive process;

2) Repeated SSVEP will result in significant visual fatigue;

3) Spontaneous MI requires rigorous prior training and has no good solution to the problem of BCI blindness.

To solve the comfort problem of conventional SSVEP stimulus paradigm based on flickers, some studies have proposed a BCI stimulus paradigm based on the steady-state motion visual evoked potential (SSMVEP) with a radial periodic motion as the stimulus material to reduce the visual fatigue of a long-term scintillation. Yan et al. [15] proved that the SSMVEP can quickly record the brain feedback of a periodic motion, and it does not show an obvious adaptation observed in the case of repeated ERP visual stimulus. SSMVEP stimulus paradigm can alleviate visual fatigue and discomfort. Although the extreme performance of SSMVEP is not as high as SSVEP, the performance degradation of SSMVEP is significantly lower than that of SSVEP with an increase in visual fatigue [16]. Additionally, to solve the BCI blindness problem of MI, certain studies began to investigate the ERD phenomenon generated by the guidance of AO and to use it in the BCI control system [17].

In the conventional SSVEP stimulation paradigm, stable visual stimuli can be encoded in the occipital lobe through flickering stimuli at different frequencies. However, this method results in a high level of fatigue and subjects cannot use it for a long time. Although SSMVEP partially alleviates visual fatigue through periodic motion, it also brings performance bottlenecks. The MI stimulation paradigm encodes corresponding stimulus results through active movement perception rhythms. However, its disadvantage lies in the long MI process, resulting in a lower information transfer rate. Therefore, although each of the three conventional stimulation paradigms has its own advantages, their disadvantages are relatively obvious. In addition, a single conventional stimulation paradigm cannot simultaneously stimulate both SSVEP and ERD phenomena, so the controllability and scalability of the encoding are weak. Based on this, this article proposes to construct a hybrid stimulation paradigm that simultaneously activates both SSVEP and ERD phenomena in the brain area through a specific stimulus material, enhancing the controllability and scalability of the encoding while improving performance and reducing fatigue.

Based on the above analysis, the present study uses the AO tasks of robotic arm movements as a hybrid visual evoked stimulus paradigm. Initially, the radial movement of the robotic arm is modulated by the sinusoidal function to match various frequencies and induce the SSMVEP. The left and right movements are encoded into different frequencies to activate hMNS to produce the ERD phenomenon. Unlike the existing stimulus paradigms that use different media to realize two or more stimulus patterns, the hybrid stimulus paradigm proposed in this paper uses radial movement of the robotic arm as a single medium to realize two different stimulus patterns, ERD and SSMVEP. These two stimulus patterns are evoked in different brain regions and can thus be used simultaneously

in the BCI control system. Overall, the contributions of this paper can be summarized as follows:

1) We propose a visual evoked stimulus paradigm based on the periodic radial movement of the robotic arm, which can induce the stable SSMVEP;

2) Based on the observation of the periodic radial movement of the robotic arm, the stable ERD phenomenon can be induced by discriminating between left or right movements;

3) Based on the comparison of the comfort and fatigue scores of various levels, the arm movement based on body (AMB) stimuli can achieve the best comfort scores and the arm movement based on itself (AMI) stimuli can achieve the best fatigue scores.

The rest of the paper can be organized as follows. Section 2 presents the subjects, visual evoked materials, experimental procedure, and EEG signals recording. Section 3 gives the EEG signals processing procedure, and the recognition method of SSMVEP and ERD. Section 4 illustrates the results of SSMVEP and ERD recognition, and the fatigue level evaluation. Section 5 and Section 6 discussed and concluded the paper.

2. Materials and Methods.

2.1. **Subjects.** Six subjects were invited to participate in the experiment, including three males and three females; the average age was (23.27 ± 1.38) years and the range was 23-25 years. We recruited subjects without prior BCI experience from among university students. As individuals in this age range have stronger and more efficient brain activation abilities, they are capable of simultaneously performing visual stimulation and action observation-assisted motor imagery, ensuring representative EEG samples are recorded during the actual experiment. All subjects were right-handed and healthy and had normal color and visual perception. None of the subjects had prior BCI experience. A written informed consent was obtained from all subjects in compliance with the Declaration of Helsinki. The data of all experimental procedures were collected according to the recommendations and guidelines for the EEG experiments.

2.2. **Visual evoked paradigm design.** This study designed the hybrid visual evoked paradigm based on the periodic radial movement of robotic arms. To ensure the precision of periodic radial movement, the "NAO robot" platform was introduced to design the humanoid robotic arm movements. This platform can decode the detailed parameters of robotic movements to enable the design of SSMVEP of different frequencies according to the refresh rate of the monitor. However, for the purpose of action observation, the existing studies only considered the ERD phenomenon without encoding the frequency of the movements according to the refresh rate of the screen. In this study, the trajectory of the robotic arm movement is encoded based on the modulation of a sinusoidal function. Assume that the frequency of the currently presented stimulus paradigm is f, the refresh rate of the presenting screen is r, and the current frame of the stimulus paradigm is i. Then, the stimulus signal of periodic robotic arm movements can be given by the following equation:

$$\phi(i) = abs\left(\sin\left(\pi * \frac{f}{2} * \left(\frac{i}{r}\right)\right)\right), \quad i = 1, 2, \ldots, 60 \tag{1}$$

According to the radial motion procedure of the Newton rings [15], the phase of the robotic arm movement is related to the stimulus signal, which is given by the following equation:

$$E = I_{\max}\left[\sin\left(\cos\left(2 * \pi * \frac{d}{\lambda} + \phi(i) * \frac{\pi}{2}\right)^2 - 0.5\right)\right] \tag{2}$$

where the constant $\lambda = 0.05$, and the matrix $d = 360*360$ cm^2, which are presented as the stimuli in the screen. The "waving" periodic movement of the robotic arm is modulated by the function $\phi(i)$. When the index in the function $\phi(i)$ is increased, the phase i increases from 0 to π, and the robotic arm movement goes from π back to 0. Figure 1 showed the robotic arm movement cycle of a single periodic stimulus. For a 10 Hz frequency of reversal robotic arm movements, a single cycle includes 10 frames. The first 5 frames correspond to the upward movement of the robotic arm, and the last 5 frames correspond to the downward movement of the robotic arm. In the comparison experiments, we have presented the SSMVEP of arm movement based on body (AMB), arm movement based on itself (AMI), and the Newton rings.

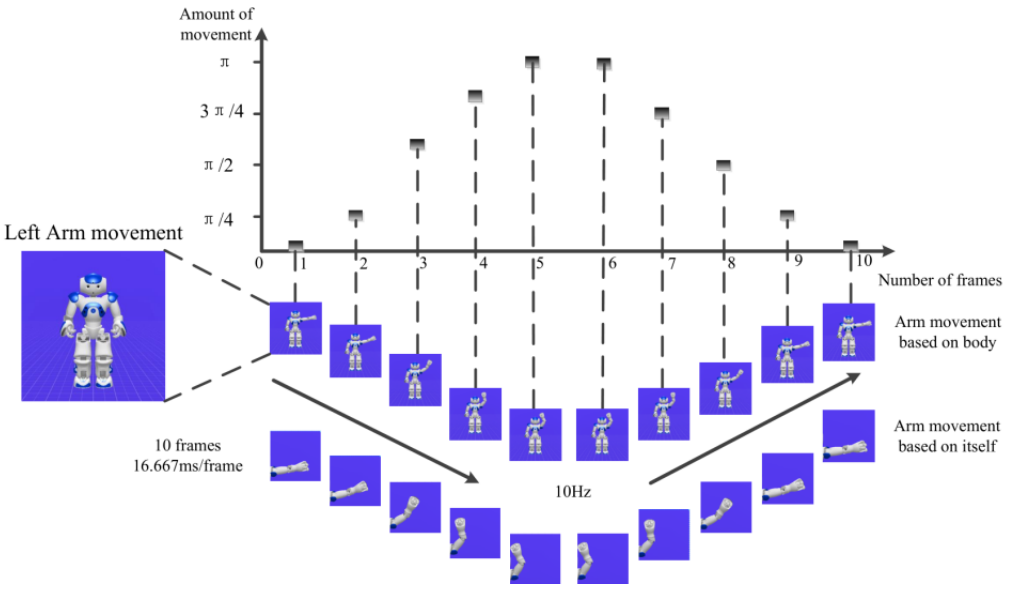

FIGURE 1. The robotic arm movement cycle of a single periodic stimulus (10 Hz)

This paper presents two types of experimental stimuli, as shown in Figure 1, both involve a waving robot motion. On the one hand, the waving motion is encoded according to a sine function, allowing the subject to induce the SSMVEP phenomenon in the occipital lobe. On the other hand, the waving motion is a typical action observation to induce the ERD phenomenon in the central lobe. During the actual experiment, we require the subject to complete the corresponding motor imagery process according to the robot's instructions. Therefore, unlike existing stimulation paradigms, we use a single stimulus material to activate both the passive SSMVEP phenomenon and the active ERD phenomenon through motor imagery. Thus, the stimulation paradigm constructed in this study has hybrid potential for constructing BCI applications.

2.3. **Experimental procedure.** During the EEG recording, each subject was seated in a comfortable armchair in front of a computer monitor in a dimly lit and sound-attenuated room. Three different groups of SSMVEP stimulus paradigms, including AMB, AMI, and the Newton rings were displayed as shown in Figure 2(a) on a DELL P2314HLCD monitor with a refresh rate of 60 frames/s. The background screen was homogeneous gray with a luminance of 38 cd/m^2, and the distance between the monitor and the subjects was set to 100 cm according to the principle of an experimental paradigm.

Each experimental paradigm consisted of six stimulus modules. Three robotic left arm movements were shown in the first line, and three robotic right arm movements were shown

in the second line. The size and position of the stimulus blocks are shown in Figure 2(a). The timing sequence of the stimulus paradigm presentation is shown in Figure 2(b). All subjects were asked to focus on one target stimulus for 4 seconds to form a trial and to rest for 2 seconds; then, the subjects selected and focused on another target stimulus for 4 seconds to form the next trial. To analyze the stable ERD phenomenon, 120 trials were included in each stimulus paradigm group, and were divided into four runs. Each run generated 30 trials, including five trials at six different frequencies. Therefore, each frequency included 20 trials for the analysis of the SSMVEP and ERD phenomena.

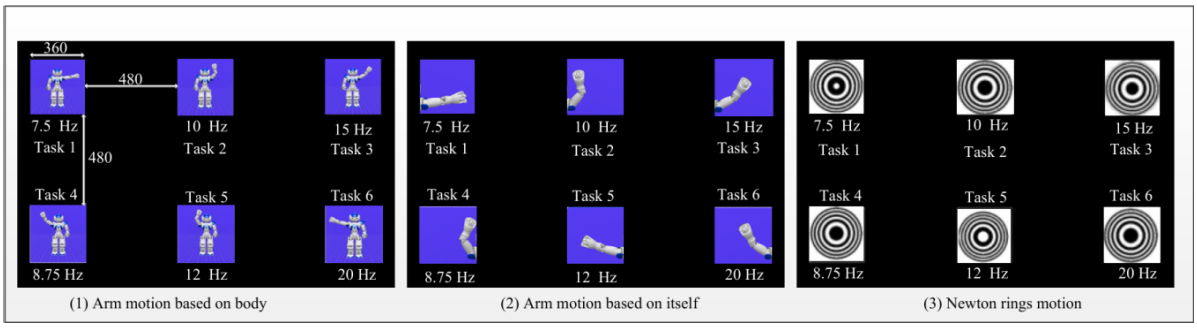

(a) Three groups of stimuli representation

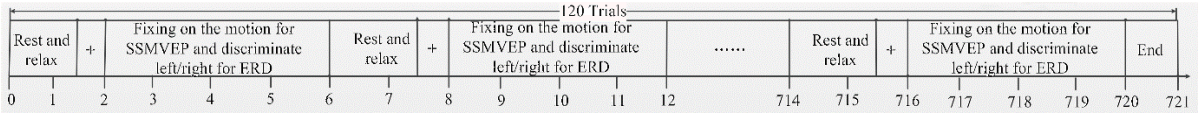

(b) Details of three groups of stimulus procedures

FIGURE 2. The presentation procedure of the stimulus paradigm

As can be seen in Figure 2(b), before each trial, there was a cross "+" clue that randomly appeared in the target stimulus and was maintained for 0.5 seconds. Then, the selected target stimulus appeared as SSMVEP and was maintained for 4 seconds. The subjects focused on the target stimulus to form a trial. Each trial was separated by a black screen for 1.5 seconds. Therefore, the rest time between two trials was 2 seconds, including 1.5 seconds break and 0.5 seconds "+" clue. Three groups of stimulus paradigms (AMB, AMI, and Newton rings) were carried out separately with a 10 minutes rest between each experiment to ensure that each type of the stimulus for the same subject did not interfere with each other.

To verify the comfort of the three stimulus groups, each subject was asked to fill in the comfort questionnaire and evaluate the visual comfort of various stimuli within 10 minutes rest after the completion of each stimulus group. Based on the four problems reported in the previous study [16], all subjects were asked to assign scores of 1-10 to the following four questions:

(A) How do you like this stimulation?
(B) How will this stimulation increase your tiredness?
(C) How long can you look at this stimulation?
(D) How annoying is this stimulation?

To ensure the fairness of the comfort score after visual stimulus presentation, three groups of visual stimuli presented by six subjects were randomly arranged in different order.

3. Data Processing and Analysis.

3.1. **Preprocessing.** After completing the experimental process and recording EEG samples from all subjects, data processing and analysis were conducted. Figure 3 illustrates the framework for EEG samples processing and analysis in this paper. First, the classical three-step approach was used for preprocessing, including filtering, baseline calibration, and sample segmentation. After preprocessing, both SSMVEP and ERD phenomena were analyzed simultaneously in this study, and the EEG from the occipital and central regions were divided into two parts. The occipital EEG was analyzed using the task-related component analysis algorithm to identify SSMVEP components, while the central EEG was analyzed using a convolutional neural network to identify ERD components. Finally, the results of SSMVEP and ERD identification were outputted for constructing a hybrid BCI.

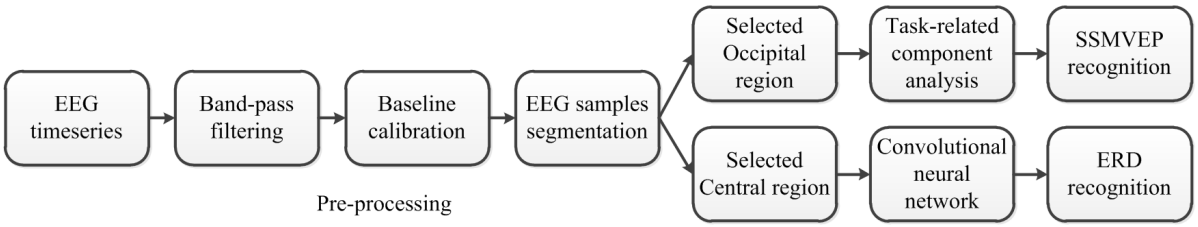

FIGURE 3. The framework for EEG samples processing and analysis

Formally, the preprocessing procedure of the recorded EEG signals used 0-40 Hz band-pass filters and 48-52 Hz notch filters. After preprocessing, the recorded labels of six different frequencies were used to define the EEG segments, and the 10% EEG signals acquired before the labeled recording time were used as the baseline to calibrate each EEG segment. Then, the recorded EOG signals were used to prevent eyeball movement and blink interference. Finally, the electrodes of *C3*, *C1*, *Cz*, *C2*, *C4*, *P3*, *P1*, *Pz*, *P2*, and *P4* were selected to recognize the ERD phenomenon, and the electrodes of *PO5*, *PO3*, *POz*, *PO4*, *PO6*, *O1*, *Oz*, and *O2* were selected to recognize the SSMVEP phenomenon. To intuitively demonstrate that the hybrid visual evoked stimulus paradigm of the robotic arm movement can produce reliable SSMVEP and ERD phenomenon simultaneously, machine learning and pattern recognition based methods were used to identify the SSMVEP and ERD phenomena at six frequencies in the three stimulus groups.

3.2. **Recognition of SSMVEP.** The recognition of SSMVEP used the latest task-related component algorithm (TRCA) [18]. Unlike the conventional canonical correlated analysis (CCA) algorithm, TRCA does not match the EEG signals collected based on a specific frequency with the signal template to find the maximum correlation coefficients. Instead, TRCA uses the optimal projection vector to find the task-related part of the EEG signals, which is more accurate and efficient for the recognition of SSMVEP. Assume that EEG signals detected by eight electrodes in the occipital region are $X(t) \in R^{N_c \times N_t}$, and the recorded signals are task-related signals $s(t) \in R$ and task-independent signals $n(t) \in R$:

$$X_i(t) = a_{i_1} s(t) + a_{i_2} n(t), \quad i = 1, 2, \ldots, N_c \tag{3}$$

where i represents the EEG-collecting electrode, and N_c represents the total number of the electrodes. a_{i_1} and a_{i_2} represent the mixed coefficients that projected from the original EEG signals to the collected EEG signals. The purpose of TRCA is to restore the task-related components using the collected EEG signals:

$$Y(t) = \sum_{i=1}^{N_c} w_i X_i(t) = \sum_{i=1}^{N_c} \left(w_i a_{i_1} s(t) + w_i a_{i_2} n(t) \right) \tag{4}$$

This recovery task can be accomplished by maximizing the covariance matrix between the trials of the EEG signals. Therefore, maximization of the covariance matrix with constrained conditions is given by the following equation:

$$\hat{w} = \arg\max_{w} \frac{w^T S w}{w^T Q w} \tag{5}$$

The optimization problem can be solved by calculating the eigen-vectors of the matrix. By sorting the eigen-values of the matrix in a descending order, the eigen-vectors corresponding to the eigen-values can be obtained as the results of the optimization problem. For recognition of the SSMVEP-BCI control system, the EEG signals of each subject were preprocessed using a filter bank. Then, for the stimulus frequency f_n, the optimal eigen-vector $w_n^{(m)} \in R^{N_c}$ can be calculated by TRCA. Finally, for each tested EEG sample from each subject, the correlation coefficient can be calculated based on the test signals and the average signals $\bar{X}_{train}^{(m)}$ of the training set:

$$r_n^{(m)} = \rho \left(\left(X_{test}^{(m)} \right) w_n^{(m)}, \left(\bar{X}_{train}^{(m)} \right) w_n^{(m)} \right) \tag{6}$$

where $\rho(\cdot)$ represents the Pearson correlation coefficient between the test EEG samples and average training samples. Similarly, TRCA needs to divide all EEG samples into a training set and a test set. In the case of the experimental data for 20 trials at each frequency, TRCA uses the leave-one-rest strategy to give the final recognition results.

3.3. **ERD recognition based on AO.** The recognition of ERD phenomenon is mainly used to classify the visual stimuli of different robotic arm movements on the left and right sides. The left and right movements were classified based on the columns in Figure 2(a) generating a total of three groups for the AMB and AMI stimulus paradigms. Newton rings do not generate ERD phenomenon. Hence, this stimulus paradigm was not included in the ERD recognition. In this study, the FBCSPnet deep learning model [19] was used to recognize the ERD phenomenon. Assuming that the EEG signals include 10 electrodes in the central region, $X^j \in R^{E \times T}$. Since only 20 trials were recorded at each frequency, there were 40 trials combining left and right movements that do not properly train the FBCSPnet model. Therefore, a cropping strategy was used to generate additional samples from 40 trials [20]. During the experiment, a single trial recorded 1,000 sampling points, and the results of the studies described in [20] indicate that stable ERD phenomenon can be produced within 2 seconds. Hence, we selected this interval as the length of a time slice, and 500 time slices were generated from one trial to form a total of 20,000 samples for the recognition of ERD.

During training of the FBCSPnet model, the error function was calculated based on the negative log of cross entropy. Assume that the time slice at t is $p_{f,k}\left(X_t^j\right)$, and the time slice at $t+T'$ is $p_{f,k}\left(X_{t,\ldots,t+T'}^j\right)$. Then, the recognition probability of the jth sample is $p\left(l_k | f\left(X_{t,\ldots,t+T'}^j; \theta\right)\right)$, where θ is the parameter of the FBCSPnet model that needs to be learned. l_k is the recognized label, and $k = 1, 2$ represent the movement of the left and right arms. Based on this definition, the loss function between the current time slice and the next time slice can be expressed as

$$loss\left(y^j, p_{f,k}\left(X_{t,\ldots,t+T'}^j\right)\right) = \sum_{k=1}^{K} -\log\left(p_{f,k}\left(X_{t,\ldots,t+T'}^j\right)\right) \times \delta\left(y^j = l_k\right)$$

$$+\sum_{k=1}^{K}-\log\left(p_{f,k}\left(X^{j}_{t,\ldots,t+T'}\right)\right)\times p_{f,k}\left(X^{j}_{t,\ldots,t+T'+1}\right) \quad (7)$$

After sufficient iterations and training of the FBCSPnet model, the optimal recognition parameter can be obtained as θ^*:

$$\theta^* = \arg\min_{\theta}\sum_{j=1}^{N} loss\left(y^j, p_{f,k}\left(X^{j}_{t,\ldots,t+T'}\right)\right) \quad (8)$$

During training of the FBCSPnet model, the Adam optimizer was used and the learning rate was set to 0.0001. The "dropout = 0.5" and "batch normalization" strategies were used to avoid the over-fitting problem, and the "early stopping" strategy was used to speed up network training and obtain the optimal parameters.

3.4. **Statistical analysis of comfort and fatigue.** The recorded EEG signals in each run were used to extract the SSMVEP trials, which were divided into four groups, including 1-30, 31-60, 61-90, and 91-120. These four groups contained stimulus presentation of variable duration and were divided into four fatigue levels, 1, 2, 3, and 4. All comfort and fatigue scores were calculated for six different frequencies of three group stimulus paradigms, and the results were normalized by averaging the scores. The average visual comfort scores were calculated using two positive questions (A) and (C) and two negative questions (B) and (D):

$$Comfort = \frac{A + (8 - B) + C + (8 - D)}{4.0} \quad (9)$$

The average fatigue scores were calculated using questions (B) and (C):

$$Fatigue = \frac{B + (8 - C)}{2.0} \quad (10)$$

The analysis results included comfort scores, recognition accuracy, fatigue scores, and recognition accuracy reduction according to various fatigue levels. The paired t-test examination was used to analyze the recognition accuracy and comfort scores of six different frequencies under three stimulus paradigms. The confidence level of statistically significant differences was set to 95% ($p < 0.05$).

4. Results.

4.1. **Recognition results of three different groups of SSMVEP stimulus paradigms.** To recognize the SSMVEP phenomenon, TRCA was used to train and test the recorded 120 trials at six different frequencies. During the training procedure, 108 trials were selected as the training set, and 12 trials were selected as the test set with a strategy of $10*10$ cross-validation. The average recognition accuracy in 10 validations was calculated as the final result. Table 1 shows the average recognition results for three groups of the SSMVEP stimulus paradigms. According to Table 1, the average recognition results of the AMI, AMB, and Newton rings are 75.32%±4.04%, 72.96%±5.56%, 75.41%±6.42%, respectively.

The significance test of the three groups of the SSMVEP stimulus paradigms indicates that the recognition accuracy of AMI is significantly higher than that of AMB and the Newton rings while there are no significant differences in recognition accuracy between AMB and the Newton rings. Figure 4 shows the average recognition results for the three groups of paradigms at each frequency. The results of Figure 4 indicate that the AMI stimulus paradigm achieves a more significant improvement in recognition accuracy at

TABLE 1. The average recognition results of three groups of SSMVEP stimulus paradigms

SSMVEP stimuli	AMB	AMI	Newton rings
Subject-1	77.40%	78.53%	78.62%
Subject-2	70.53%	71.40%	71.87%
Subject-3	72.07%	75.33%	74.86%
Subject-4	64.27%	69.86%	65.63%
Subject-5	80.20%	80.27%	84.63%
Subject-6	73.27%	76.53%	76.86%
Average	72.96%	75.32%	75.41%
Std	5.56%	4.04%	6.42%
Paired t-test	–	$p < 0.05$	$p < 0.01$

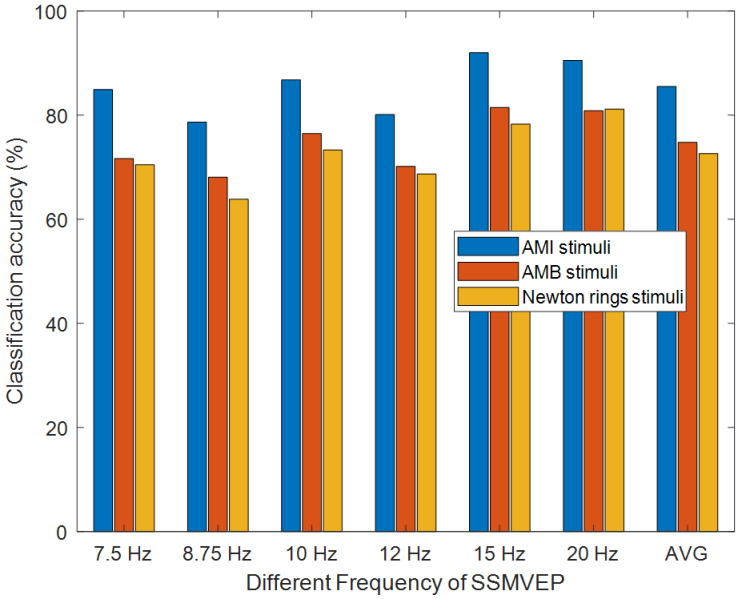

FIGURE 4. The average recognition results of the three groups of paradigms at each frequency

almost all frequencies, and the recognition accuracies of AMB and the Newton rings have only small differences at each frequency.

An additional important index, information transfer rate (ITR), was compared between the three groups of the SSMVEP stimulus paradigms. Assume the recognition rate is p, the presentation time is T, and the number of total frequencies is N, the equation for calculation of ITR is as follows:

$$ITR = \frac{60}{T}\left[\log_2 N + p\log_2 p + (1-p)\log_2\left(\frac{1-p}{N-1}\right)\right] \tag{11}$$

In general, the recognition accuracy will be improved with an increase in the presentation time. However, an increase in the presentation time will also reduce the ITR. Therefore, eight presentation time points, $T = 0.5, 1, 1.5, 2, 2.5, 3, 3.5, 4$, were used to compute the corresponding recognition accuracy and ITR. Figure 5 illustrates the accuracy and ITR at various time points. The results of Figure 5 indicate that the best recognition accuracy (71.22%) of AMB is at $T = 4$, and the best ITR (36.79 bits/min) of AMB is at $T = 1$. In addition, the best recognition accuracy (81.63%) of AMI is at $T = 4$, and the best ITR (46.09 bits/min) of AMI is at $T = 1$. Furthermore, the best recognition

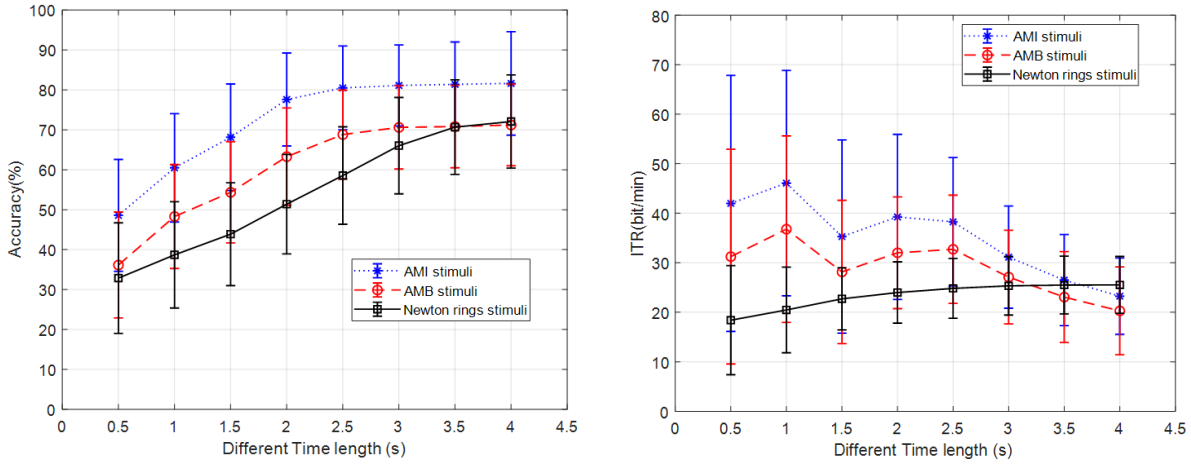

(a) Accuracy (b) ITR

FIGURE 5. The accuracy and ITR of the three SSMVEP stimulus paradigms at various time points

accuracy (72.08%) of the Newton rings is at $T = 4$, and the best ITR (25.53 bits/min) of the Newton rings is at $T = 4$.

Analysis of the recognition accuracy at various time points indicates that all three SSMVEP stimulus paradigms show an increase in discipline concomitant to an increase in the presentation duration. The arm movement-based SSMVEP stimulus paradigms have a flat trend at longer presentation duration ($T > 2$), while the conventional Newton rings SSMVEP stimulus paradigm has a stable increasing trend. Analysis of ITR at various time points indicates that arm movement-based SSMVEP stimulus paradigms have an oscillation trend at shorter presentation duration ($T \leq 2$) and a general decrease at longer presentation duration ($T > 2$). However, the conventional Newton rings SSMVEP stimulus paradigm also has a plateau trend at higher values of the ITR index.

4.2. **Recognition results of ERD for the arm movement-based stimulus paradigms.** To verify the ERD phenomenon, the periodic movements of the robotic left arm and right arm were classified and recognized as a set of samples. Each group of the stimuli paradigms included 20,000 time slice samples for training and testing. FBCSPnet was used to train a model to discriminate the movements of the left arm and right arm. The ERD phenomenon can be reflected by the classification accuracy of the testing samples. Table 2 illustrates the classification accuracy and the ERD phenomenon. The results of Table 2 indicate that the classification accuracy of AMB is higher than that detected in the case of the AMI stimulus paradigm. Specifically, the AMB stimulus paradigm at 15 Hz (left) + 20 Hz (right) has significantly improved the classification accuracy compared to that detected in the case of the AMI stimulus paradigm ($p < 0.05$). On the other hand, the AMI stimulus paradigm is not strong enough to activate hMNS due to its poor humanness. These results provided a certain reference significance for the subsequent studies of action observation guided MI. In the case of the paradigm based on a humanoid robot, the presentation of the whole "humanoid" body is more conductive to the stimulation of the hMNS feedback to action observation guided MI.

4.3. **Evaluation of the visual comfort and fatigue for the SSMVEP stimulus paradigms.** Table 3 illustrates the scores of visual comfort questionnaire. The visual comfort is higher for the periodic radial movement of robotic arm compared with that

TABLE 2. ERD classification results for left and right arm movements for AMI and AMB

AO tasks	Left-7.5 Hz	Right-8.75 Hz	Left-10 Hz	Right-12 Hz	Left-15 Hz	Right-20 Hz
Stimuli	a: AMI	b: AMB	c: AMI	d: AMB	e: AMI	f: AMB
Subject-1	70.58%	64.56%	81.12%	77.23%	61.16%	67.62%
Subject-2	77.54%	77.45%	71.65%	60.42%	66.48%	76.93%
Subject-3	71.48%	86.83%	76.52%	84.28%	64.56%	74.13%
Subject-4	72.31%	83.29%	80.83%	85.19%	70.87%	65.65%
Subject-5	70.68%	87.64%	67.12%	86.87%	63.54%	75.79%
Subject-6	77.83%	73.45%	76.86%	75.23%	64.88%	74.94%
Average	73.40%	78.87%	75.68%	78.20%	65.25%	72.51%
Standard deviation	3.38%	8.90%	5.44%	9.87%	3.27%	4.69%
ITR (bits/min)	4.65	7.65	6.23	7.29	1.87	4.84
Paired t-test	a vs. b	$p = 0.246$	c vs. d	$p = 0.590$	e vs. f	$p < 0.05$

TABLE 3. The average scores of visual comfort questionnaire

Stimuli	A	B	C	D	Comfort	Fatigue
AMI	6.50	5.17	5.67	5.00	5.75	5.25
AMB	7.67	3.17	7.33	2.82	7.75	3.42
Newton rings	4.83	6.83	3.83	6.33	4.37	7.00
Average	6.33	5.06	5.61	4.72	5.96	5.22
Standard deviation	1.43	1.83	1.75	1.77	1.70	1.79

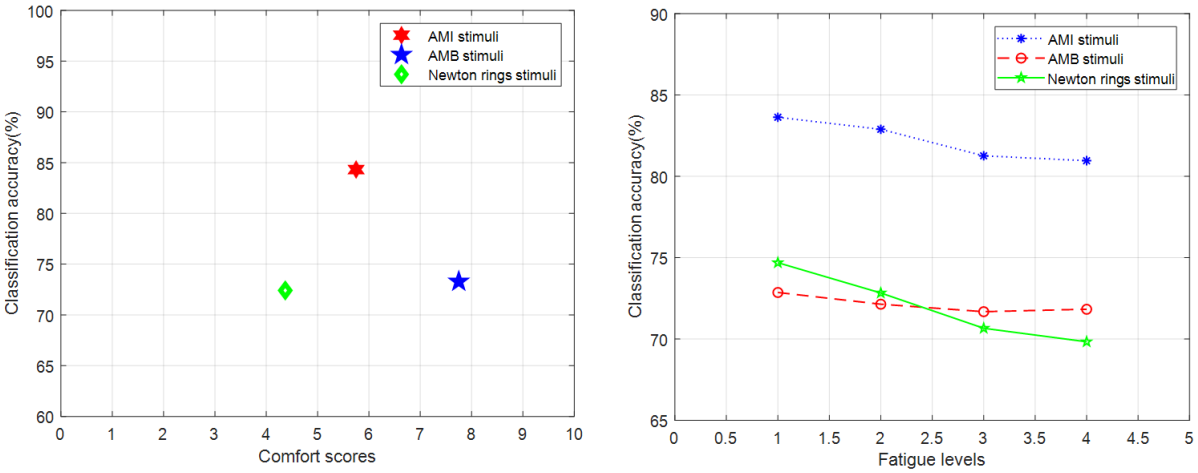

(a) Comfort scores (b) Fatigue levels

FIGURE 6. The relationship between recognition accuracy and visual comfort and fatigue levels

for the Newton rings. However, the differences in the visual comfort between AMI and AMB are not significant. The AMB stimulus paradigm achieves the best visual comfort apparently because the presentation form includes the whole "humanoid" body. Figure 6(a) shows the comparative relationship between the visual comfort and the recognition accuracy. The horizontal axis and the vertical axis represent the average comfort score and the average recognition accuracy of all six subjects, respectively. The results of Figure 6

indicate that the AMB stimulus paradigm has a comfort advantage over that of the conventional Newton rings, and the AMI stimulus paradigm has a recognition accuracy advantage over that of the conventional Newton rings. Two robotic arm movement-based hybrid stimulus paradigms have better advantages.

Long-term use of the SSMVEP-BCI control system will cause greater visual fatigue. Based on the presentation duration and fatigue levels (1, 2, 3, and 4), the TRCA algorithm was used to classify the trials to four fatigue levels. Figure 6(b) shows the SSMVEP recognition accuracy under various fatigue levels. The results of Figure 6 indicate that all three groups of the SSMVEP stimulus paradigms have a trend of a decrease in the recognition accuracy concomitant to an increase in the fatigue level. The decrease is the highest in the Newton rings stimulus paradigm (1.03%) followed by the AMI stimulus paradigm (2.67%), and the AMB stimulus paradigm induced the lowest decrease (4.86%).

According to the results in Table 3, both the AMI and AMB stimuli materials constructed in this study have higher comfort and lower fatigue levels than the conventional Newton rings SSMVEP stimuli material. In fact, the Newton rings SSMVEP stimuli material is significantly superior to the fatigue and discomfort caused by traditional flicker stimuli materials. Therefore, long-term use of the AMI and AMB stimuli materials will not cause significant fatigue problems for the subjects. In addition, compared to a single type of stimulus material, the stimulus material constructed in this study simultaneously activates both the ERD and SSMVEP phenomena, enabling a more diverse range of encoding schemes to be combined and enriching the practical application scenarios of hybrid BCI. For example, when using BCI technology to control the fingers of a robot with high precision, it is not possible to control all 20 joints of the 5 fingers with just motor imagery. If the AMI/AMB stimulation paradigm constructed in this study is used, 20 joint control instructions can be easily encoded by relying on 5 sets of SSMVEP commands and 4 sets of ERD commands, achieving the goal of precise robot control.

5. **Discussion.** The purpose of the hybrid visual stimulus paradigm is to use two or more materials to evoke multiple brain phenomena. The commonly used hybrid paradigm is combined with SSVEP based on flickers, P300 based on screening stimulus, and ERD based on MI. In this study, two brain phenomena, SSMVEP and ERD, were simultaneously generated by the periodic radial robotic arm movement of the visual stimulus paradigm. Such two phenomena were verified based on the spectral power and recognition accuracy. Previous studies have shown that two parallel primary pathways are presented in the human visual system [21], including the shape and color perception pathway and the movement perception pathway. The periodic radial movements of the robotic arms cause the perception process of the spatial motion of the visual system, and the repeated observation induces the stable SSMVEP phenomenon. Additionally, the robotic arm movements can be observed, and the left movement can be discriminated from the right movement. During the observation and discrimination, the visual system in the brain further activates the hMNS, and the ERD phenomenon in the contralateral brain region can be generated due to the action observation guided MI [22]. Since these two different phenomena are located in different brain regions, including the ERD phenomenon in the parietal region and the SSMVEP in the occipital region, the signals can be analyzed simultaneously.

Assuming that the SSMVEP-BCI control system contains N frequencies with the left and right commands from the ERD phenomenon, the hybrid stimulus paradigm can be used to generate $2 \times N$ control signals. Additional commands will improve the ITR of the BCI control system. The recognition accuracy results of Table 1 and Table 2 indicate that the recognition accuracy of SSMVEP (75.41%) is slightly higher than that of the ERD

phenomenon (72.51%). The combination of SSMVEP and ERD will reduce the recognition rate to (65.25%) after doubling the commands. Therefore, our further studies will investigate how these two phenomena can be reasonably combined to obtain more stable and higher ITR. Additionally, the highest ITR of SSMVEP duration is concentrated in the range from 1 to 1.5 s, and ERD is generally believed to require continuous presentation for 2 s. Time matching between these two phenomena is another direction for our future studies. Finally, action observation guided MI should be included in a visual evoked stimulus paradigm. Relevant studies [23,24] on action observation guided MI have shown that the hMNS activation produces power variations in the occipital region concentrated in the alpha and beta rhythms. Additional studies are needed to determine the presence of coupling between the SSMVEP and ERD phenomenon in the occipital region during the visual stimulus presentation of the periodic radial movement, and solutions of the coupling of the mutually restricted phenomena are required.

Comparison of the recognition accuracy of the SSMVEP stimulus paradigm in three groups indicates that the AMB stimulus paradigm achieves the highest accuracy in the case of the ERD phenomenon, and the AMI stimulus paradigm achieves the highest accuracy in the case of SSMVEP. The two stimulus paradigms proposed in this study have certain advantages over the Newton rings. The recognition accuracy of the AMB stimulus paradigm in SSMVEP is not substantially different from that of the Newton rings. However, the ERD phenomenon, which is not available in the Newton rings, can generate more commands and improve the ITR of BCI [25]. However, the recognition accuracy of the AMI stimulus paradigm is significantly higher than that of the Newton rings although the recognition of the ERD phenomenon is relatively general. The comfort scores shown in Table 3 and Figure 6(a) indicate that the stimulus paradigms based on the periodic radial robotic arm movements have better comfort scores than those of the conventional Newton rings, which are essentially consistent with the comfort degree of the radial zoom motion-based stimulus paradigm. However, the overall recognition is limited by coupling of various visual stimulus phenomena, and the recognition accuracy of SSMVEP cannot achieve the results of the radial zoom motion (93.41%). Complex visual stimulus phenomena were detected in the robotic-based paradigm, and various factors, such as humanoid shape, posture, and color, are all needed to be considered. The current design of the robotic arm periodic radial movement is relatively simple. Design of a more complex periodic movement mode of the robotic arm will produce different brain phenomena, which is the next step of our studies.

When the visual evoked stimulus paradigm is used to construct the BCI control system, the visual fatigue and adaptability caused by a long-term visual attention will inevitably lead to the weakened process of visual feedback [26]. Therefore, an increase in the presentation time of the visual stimulus paradigm suggests that the stimulus paradigm with an insignificant decrease in recognition accuracy is more suitable for construction of the BCI control system. In this study, two hybrid visual evoked stimulus paradigms are proposed to build the BCI control system. Such paradigms have a lower recognition accuracy compared with that of the conventional Newton rings. This decrease is due to an increase in the visual fatigue levels. The AMB stimulus paradigm has the lowest accuracy decrease, which has the advantage of being an overall "whole" when used for a long-term presentation, and the fatigue of this paradigm accumulates more slowly than the "part" type stimulus paradigm, which is potentially instructive due to the degradation in performance induced by an increase in the fatigue levels. How to design a more objective fatigue evaluation standard in the construction of a real-world BCI control system, how to design a personalized "humanoid robot" according to individual fatigue evaluation situation, and how to implement a personalized hybrid visual evoked stimulus paradigm are the three

key problems related to the hybrid evoked stimulus paradigm based on the robotic arm periodic radial movement. Such problems will be considered in our further studies.

From the experimental results of the stimulus materials designed in this study, it can be seen that the AMI is more suitable for passively inducing the SSMVEP phenomenon in the subjects, while the AMB is more suitable for actively inducing the ERD phenomenon in the subjects. Therefore, one limitation of the stimulus materials is the inability to combine the advantages of AMI and AMB, resulting in better adaptability in the activation modes of the two brain regions. Another limitation of the stimulus materials is the issue of recognition accuracy. Among the 6 subjects recruited for the experiment in this study, the recognition accuracy of both the ERD and SSMVEP phenomena was only about 70%, which is only sufficient for constructing a simple hybrid BCI system. If we want to combine the encoding instructions of ERD and SSMVEP to construct a more precise control instruction set, such as non-holonomic wheeled mobile robots control [27], the existing 70% accuracy is far from enough. Combining the instructions will gradually amplify the misidentified instructions, reducing the performance of the BCI system. Therefore, future research needs to construct higher-performance decoding algorithms for ERD and SSMVEP to achieve higher recognition performance and meet the performance indicators of constructing online hybrid BCI.

6. **Conclusion.** In this study, we proposed a novel hybrid evoked stimulus paradigm based on the robotic arm periodic radial movement, and the experimental results have demonstrated that this paradigm simultaneously generates the SSMVEP and ERD phenomena. Two visual stimulus paradigms were tested: AMB can achieve higher recognition accuracies of the ERD phenomenon, and AMI can achieve higher recognition accuracies of the SSMVEP. The recognition accuracy results indicate that the proposed stimulus paradigms can be potentially combined to generate multiple commands for the BCI control system. The comfort analysis results obtained after the experiment have shown that the proposed paradigms have better comfort degree than the conventional Newton rings, and the AMB stimulus paradigm has the highest comfort degree, which has the least impact on a decrease in the recognition accuracy due to an increase in the visual fatigue levels. This hybrid visual evoked paradigm has good characteristics. However, further studies are necessary to solve the coupling problem of the SSMVEP and ERD phenomenon in the occipital region, design more complex movement patterns of the robotic arm, and refine the objective fatigue evaluation method to implement a personalized stimulus paradigm.

Acknowledgement. This work was supported by the Fuzhou Polytechnic research foundation (No. FZYKJJJJC202001). The funding body played the role in supporting the experiments. The author is very grateful to the anonymous reviewers for their constructive comments which have helped significantly in revising this work.

REFERENCES

[1] M. A. Lebedev and M. A. Nicolelis, Brain machine interfaces: Past, present and future, *Trends in Neurosciences*, vol.29, no.9, pp.536-546, 2006.

[2] M. A. Lebedev, Brain-machine interfaces: An overview, *Translational Neuroscience*, vol.5, no.1, pp.99-110, 2014.

[3] R. Abiri, S. Borhani, E. W. Sellers, Y. Jiang and X. Zhao, A comprehensive review of EEG-based brain computer interface paradigms, *Journal of Neural Engineering*, vol.16, no.1, 011001, 2019.

[4] H. Lin and J. Liang, Contextual effects of angry vocal expressions on the encoding and recognition of emotional faces: An event-related potential (ERP) study, *Neuropsychologia*, vol.132, 107147, 2019.

[5] R. Land, A. Kapche, L. Ebbers and A. Kral, 32-channel mouse EEG: Visual evoked potentials, *Journal of Neuroscience Methods*, vol.325, 108316, 2019.
[6] M. Gong, G. Xu, M. Li and F. Lin, An idle state-detecting method based on transient visual evoked potentials for an asynchronous ERP-based BCI, *Journal of Neuroscience Methods*, vol.337, 108670, 2020.
[7] Z. Lin, C. Zhang, W. Wu and X. Gao, Frequency recognition based on canonical correlation analysis for SSVEP-based BCIs, *IEEE Transactions on Biomedical Engineering*, vol.53, no.12, pp.2610-2614, 2006.
[8] J. Yordanova, V. Kolev and J. Polich, P300 and alpha event-related desynchronization (ERD), *Psychophysiology*, vol.38, no.1, pp.143-152, 2001.
[9] H. Nagai and T. Tanaka, Action observation of own hand movement enhances event-related desynchronization, *IEEE Transactions on Neural Systems and Rehabilitation Engineering*, vol.27, no.7, pp.1407-1415, 2019.
[10] T. Yu, J. Xiao, F. Wang, R. Zhang, Z. Gu, A. Cichocki and Y. Li, Enhanced motor imagery training using a hybrid BCI with feedback, *IEEE Transactions on Biomedical Engineering*, vol.62, no.7, pp.1706-1717, 2015.
[11] M. Wang, I. Daly, B. Z. Allison, J. Jin, Y. Zhang, L. Chen and X. Wang, A new hybrid BCI paradigm based on P300 and SSVEP, *Journal of Neuroscience Methods*, vol.244, pp.16-25, 2015.
[12] Y. Yu, Z. Zhou, Y. Liu, J. Jiang, E. Yin, N. Zhang and D. Hu, Self-paced operation of a wheelchair based on a hybrid brain-computer interface combining motor imagery and P300 potential, *IEEE Transactions on Neural Systems and Rehabilitation Engineering*, vol.25, no.12, pp.2516-2526, 2017.
[13] Z. Wang, Y. Yu, M. Xu, Y. Liu, E. Yin and Z. Zhou, Towards a hybrid BCI gaming paradigm based on motor imagery and SSVEP, *International Journal of Human Computer Interaction*, vol.35, no.3, pp.197-205, 2019.
[14] S. Machado, F. Arajo, F. Paes, B. Velasques, M. Cunha, H. Budde and R. Piedade, EEG-based brain-computer interfaces: An overview of basic concepts and clinical applications in neuro-rehabilitation, *Reviews in the Neurosciences*, vol.21, no.6, pp.451-468, 2010.
[15] W. Yan, G. Xu, M. Li, J. Xie, C. Han, S. Zhang and C. Chen, Steady-state motion visual evoked potential (SSMVEP) based on equal luminance colored enhancement, *PloS One*, vol.12, no.1, e0169642, 2017.
[16] X. Chai, Z. Zhang, K. Guan, G. Liu and H. Niu, A radial zoom motion-based paradigm for steady state motion visual evoked potentials, *Frontiers in Human Neuroscience*, vol.13, 127, 2019.
[17] T. J. Luo, J. Lv, F. Chao and C. Zhou, Effect of different movements speed modes on human action observation: An EEG study, *Frontiers in Neuroscience*, vol.12, 219, 2018.
[18] M. Nakanishi, Y. Wang, X. Chen, Y. T. Wang, X. Gao and T. P. Jung, Enhancing detection of SSVEPs for a high-speed brain speller using task-related component analysis, *IEEE Transactions on Biomedical Engineering*, vol.65, no.1, pp.104-112, 2018.
[19] R. T. Schirrmeister, J. T. Springenberg, L. D. J. Fiederer, M. Glasstetter, K. Eggensperger, M. Tangermann and T. Ball, Deep learning with convolutional neural networks for EEG decoding and visualization, *Human Brain Mapping*, vol.38, no.11, pp.5391-5420, 2017.
[20] T. Luo, C. Zhou and F. Chao, Exploring spatial-frequency-sequential relationships for motor imagery classification with recurrent neural network, *BMC Bioinformatics*, vol.19, no.1, 344, 2018.
[21] R. Gatti, M. A. Rocca, S. Fumagalli, E. Cattrysse, E. Kerckhofs, A. Falini and M. Filippi, The effect of action observation/execution on mirrorneuron system recruitment: An fMRI study in healthy individuals, *Brain Imaging and Behavior*, vol.11, no.2, pp.565-576, 2017.
[22] A. Dionísio, R. Gouveia, I. C. Duarte, J. Castelhano, F. Duecker and M. Castelo-Branco, Continuous theta burst stimulation increases contralateral mu and beta rhythms with arm elevation: Implications for neurorehabilitation, *Journal of Neural Transmission*, vol.127, no.1, pp.17-25, 2020.
[23] A. Koul, A. Cavallo, F. Cauda, T. Costa, M. Diano, M. Pontil and C. Becchio, Action observation areas represent intentions from subtle kinematic features, *Cerebral Cortex*, vol.28, no.7, pp.2647-2654, 2018.
[24] N. Brihmat, M. Tarri, Y. Quidé, K. Anglio, B. Pavard, E. Castel-Lacanal and I. Loubinoux, Action, observation or imitation of virtual hand movement affect differently regions of the mirror neuron system and the default mode network, *Brain Imaging and Behavior*, vol.12, no.5, pp.1363-1378, 2018.
[25] X. Zhu, P. Li, C. Li, D. Yao, R. Zhang and P. Xu, Separated channel convolutional neural network to realize the training free motor imagery BCI systems, *Biomedical Signal Processing and Control*, vol.49, pp.396-403, 2019.

[26] X. Zheng, G. Xu, Y. Zhang, R. Liang, K. Zhang, Y. Du and S. Zhang, Anti-fatigue performance in SSVEP-based visual acuity assessment: A comparison of six stimulus paradigms, *Frontiers in Human Neuroscience*, vol.14, 301, 2020.

[27] S. Wan, Y. Zhang, Z. He and L. Chen, Periodic event-triggered tracking control for nonholonomic wheeled mobile robots, *International Journal of Innovative Computing, Information and Control*, vol.18, no.5, pp.1507-1517, 2022.

Author Biography

Minghua Wei received the Ph.D. degree from the College of Agriculture, Fujian Agriculture and Forestry University, Fuzhou, China, in 2017. He is currently working as a professor at the Department of Information Engineering, Fuzhou Polytechnic, Fuzhou, China. His research interests include computer vision, machine learning, brain computer interface, and artificial intelligence in medicine.